Biophysical Chemistry, 49 (1994) 141–152
Elsevier Science B.V., Amsterdam

BIOCHE 1811

Calculation of the circular dichroism spectrum of cyclo-(L-tyr-L-tyr) based on a molecular dynamics simulation

Jörg Fleischhauer [a], Joachim Grötzinger [b], Bernd Kramer [a], Peter Krüger [b], Axel Wollmer [b], Robert W. Woody [c,*] and Elke Zobel [a]

[a] *Institute of Organic Chemistry, Rheinisch-Westfälische Technische Hochschule, Aachen (Germany)*
[b] *Institute of Biochemistry, Rheinisch-Westfälische Technische Hochschule, Aachen (Germany)*
[c] *Department of Biochemistry and Molecular Biology, Colorado State University, Fort Collins, CO 80523 (USA)*

(Received 26 April 1993; accepted in revised form 18 August 1993)

Abstract

Theoretical calculations of CD spectra have generally assumed a single conformation, or a small number of conformers with Boltzmann averaging. Solvent effects on both the conformation and the CD have been neglected. In this work, we have calculated the CD spectrum of cyclo(L-Tyr-L-Tyr) in aqueous solution, taking dynamics and solvation into account. Starting geometries with $\chi_1 \approx 300°$ or 60° for both Tyr side chains were derived from MNDO/MOPAC, followed by energy minimization using GROMOS. After addition of 368 water molecules, the system was simulated for 1000 ps at 300 K using GROMOS. In addition to the starting conformer, two other conformers were observed during each simulation. However, each trajectory gave a distinct set of conformers. Rotational strengths were calculated for the cyclic dipeptide at each ps along the trajectories, using the matrix method. The CD spectra calculated from these rotational strengths were averaged over the trajectories. Agreement is very good for the strong negative band near 200 nm, while for the lower energy bands (near 230 and 280 nm), the signs are correct, but the magnitudes are too low. The spectrum calculated from a Boltzmann-weighted average over the *in vacuo* MNDO/MOPAC conformers was in poor agreement with experiment. Although the solvent did not significantly affect the rotational strength calculated for a given conformer, it is essential to include the solvent in the MD simulations because it affects the relative energies of the conformers and promotes transitions among them.

Keywords: Circular dichroism; Molecular dynamics; Cyclic dipeptide; Tyrosine; Solvent effect; Diketopiperazine

1. Introduction

Calculations of the circular dichroism spectra of molecules have generally considered only one (or a few) conformation(s) of an isolated molecule. In other words, the effects of dynamics and of solvation have been neglected. It is not clear to what extent the neglect of these factors may compromise the results of rotational strength calculations. It is now possible to carry out realistic simulations of molecules in aqueous solution using the technique of molecular dynamics [1–3]. In this paper, we describe calculations of the CD spectrum of a cyclic dipeptide based upon a

* Corresponding author.

SSDI 0301-4622(93)E0065-D

molecular dynamics trajectory. The simulations have been performed in aqueous solution.

We have chosen cyclo (L-Tyr-L-Tyr), denoted as cYY, as our model system and test case. There are several reasons for this choice. Cyclic dipeptides (diketopiperazines or, more correctly, piperazinediones) [4,5] have long been favored as models for spectroscopic studies of peptide systems because they exhibit the effects of amide-amide interactions at the dimer level and because they are relatively (but not completely) well-defined in conformation. The presence of the two aromatic side chains in cYY makes this system of special interest for modeling the effects of aromatic groups coupled with peptides. In fact, the one previous study [6] in which dynamic effects were considered in calculations of CD dealt with the side-chain CD bands of insulin, due to tyrosyl groups.

Extensive theoretical and experimental studies have been reported on the CD of cYY [7–9] as well as other cyclic dipeptides with one or two aromatic side chains [10–12]. In the conformational energy calculations of Snow et al. [9], only the side-chain torsional angles, χ_1 and χ_2, and an angle β [13] describing the folding of the diketopiperazine ring were considered. They identified six local minima, with the global minimum corresponding to $\beta = 0°$ (planar piperazinedione ring), with one tyrosyl side chain having $\chi_1 = 60°$ (folded over the piperazinedione ring) and the other with $\chi_1 = 300°$ (an extended conformation). They calculated the rotational strengths for each of the minimum-energy conformers and used Boltzmann weighting factors based upon the potential energy to calculate the average rotational strengths for the side-chains and backbone transitions.

The CD curve calculated [9] from these conformationally averaged rotational strengths accurately reproduced the sign of the three CD bands which were unambiguously determined (Fig. 1). Snow et al. did not explicitly assign the peptide $n\pi^*$ transition because they were unable to obtain a consistent fit for this transition to the CD curves observed in neutral and basic aqueous solution, trimethylphosphate and methanol. However, it seems likely that the negative maximum

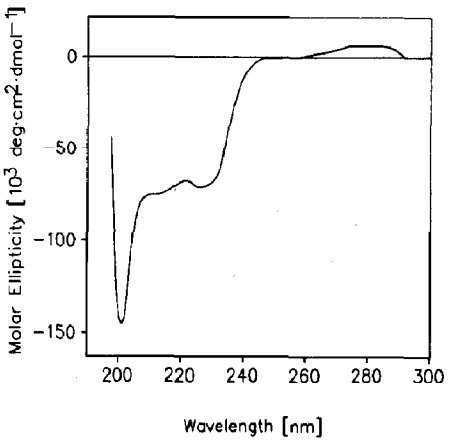

Fig. 1. Experimental CD spectrum of cYY in neutral aqueous solution, as reported by Snow et al. [9].

observed near 215 nm in neutral aqueous solution is the $n\pi^*$ band. If so, the averaged rotational strength was incorrect in sign for this band. Snow et al. compared their calculated spectrum to that obtained in trimethylphosphate because this was the least polar solvent they used, and their calculations assumed a unit dielectric constant. The calculated CD underestimated the long-wavelength L_b band intensity by about a factor of two, gave reasonable agreement with the L_a band near 230 nm, and overestimated the 200 nm band by approximately a factor of two.

2. Methods

2.1. Starting geometries

Six starting conformers were generated, corresponding to all distinguishable combinations of torsional energy minima for the variable χ_1 at each of the two residues. These minima are designated by the χ_1 values: (60, 60), (180, 60), (180, 180), (300, 60), (300, 180) and (300, 300). A side chain for which $\chi_1 = 60°$ is in a folded conformation, with the phenolic ring located above the piperazinedione ring. For $\chi_1 = 180°$, the phenolic ring is extended away from the piperazinedione, toward the carbonyl group of the residue. In conformers with $\chi_1 = 300°$ the phenolic group is also extended, but toward the NH side of C^α. In

all cases, the piperazinedione ring was planar and χ_2 was taken to be 90°. Each of the six starting geometries was subjected to energy minimization by MNDO/MOPAC [14]. The lowest and highest energy conformers, (300, 300) and (60, 60), respectively, were then subjected to energy minimization using the GROMOS force field [15] and the method of steepest descents [16], until the total energy change between successive steps was less than 0.01 kJ/mol.

2.2. Molecular dynamics simulations

Two simulations were performed at 300 K using the GROMOS program library [15]. The starting geometries for cYY were the energy-minimized conformers (300, 300) and (60, 60), the lowest and highest energy conformers *in vacuo*, according to the MNDO calculations. The molecules were placed in a truncated octahedral box of dimensions $a = 28.5$ Å with 368 SPC [17] water molecules, thermally equilibrated at 300 K, and energy minimized.

Initial velocities for the atoms were generated at random, according to a Maxwell–Boltzmann distribution at 300 K. Bond lengths were constrained using the SHAKE algorithm [18] and a time step of 2 fs was used. A cutoff radius of 9.5 Å was used for the Lennard-Jones and Coulomb terms. The molecules were weakly coupled to a thermal bath at $T = 300$ K [19], with a temperature relaxation time $\tau = 0.1$ ps. Periodic boundary conditions were used. After an equilibration period of 10 ps, the simulations were carried out for 1000 ps, with the structures recorded every ps for analysis.

One simulation at high temperature was conducted to test whether a broader range of conformers could be observed in a single simulation. The temperature chosen was 600 K. The starting geometry was a (300, 60) conformer corresponding to the 600 ps point in the second simulation mentioned above (starting with the (60, 60) conformer at 300 K and with 368 SPC water molecules). A new set of randomly chosen velocities with a Maxwellian distribution corresponding to 600 K was assigned to the solute and solvent atoms, the system was coupled to a 600 K bath with a coupling constant of 0.1 ps, and a time step of 2 fs was used. The pressure was held constant, allowing the volume of the box to expand roughly tenfold over the course of the simulation, which was carried out for 130 ps.

2.3. Rotational strength and CD calculations

Rotational strengths were calculated by the matrix method [20] for each structure recorded along the two MD trajectories, using programs written by Zobel [21] and Kramer [22]. The matrix elements coupling transitions in different groups and mixing excited states within individual chromophores were calculated using the monopole–monopole approximation [23].

The monopole positions and charges were obtained by numerical integration [22] over CNDO/2s [24] wavefunctions for the molecules formamide and phenol, which represent the interacting chromophores in cYY. This method and resulting monopole positions and charges will be described in more detail elsewhere (Kramer et al., to be published).

In another set of calculations, the monopoles just described were supplemented by a set of monopoles intended to take account of vibronic intensity contributions for the L_b and L_a [25] bands of the phenolic group. These vibronic monopoles have been described previously [26] and will be presented in detail elsewhere (Sreerama et al., to be published).

In addition to the monopole charges and positions, required to calculate the off-diagonal elements, the electric and magnetic transition dipole moments and the transition energies for the isolated chromophores must also be specified. The transition dipole moments were taken from CNDO/2s calculations on the model chromophores.

The monopole positions of both chromophores are defined with respect to the structure of the isolated groups saturated with H atoms and energy minimized by MNDO/MOPAC [14]. These structures were fitted to the structure from the MD trajectory using a least-squares method [27]. The resulting transformation vectors and rotational matrices were then used to calculate the

new monopole positions and the electric and magnetic moment vectors.

The static field which mixes excited states within each chromophore was calculated using monopoles evaluated from the ground-state wavefunctions. In one set of calculations, permanent charges were placed on the solvent molecules as well as on the solute. The charges used for the solvent atoms were those for SPC [17] water, as used in the MD simulation.

CNDO/2s calculations indicate that several magnetically allowed transitions ($\sigma\pi^*$ and $\pi\sigma^*$) occur at energies similar to or just higher than those of the electrically allowed B transitions of phenol. One set of calculations was performed which included the effects of mixing of these

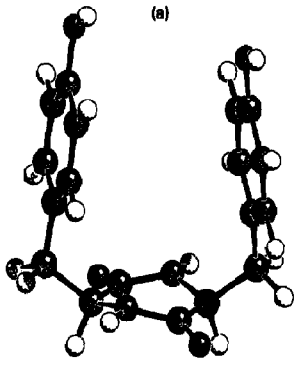

Conformer 60°/60° (-478.66 kJ/mol)

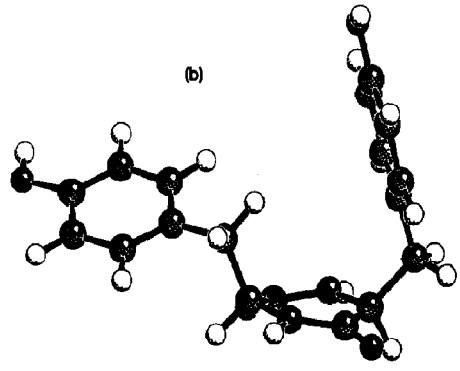

Conformer 180°/60° (-483.53 kJ/mol)

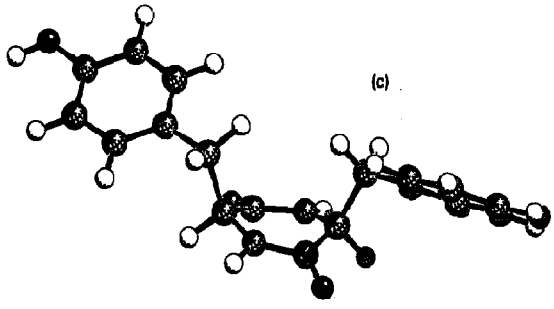

Conformer 180°/180° (-484.21 kJ/mol)

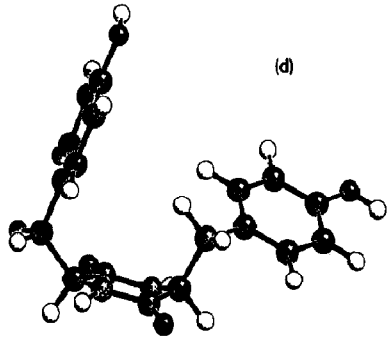

Conformer 300°/60° (-486.34 kJ/mol)

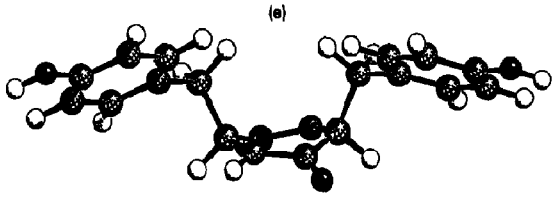

Conformer 300°/180° (-488.10 kJ/mol)

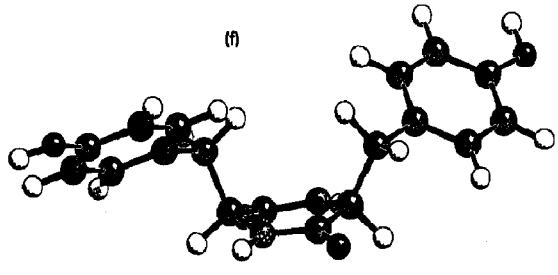

Conformer 300°/300° (-492.10 kJ/mol)

Fig. 2. Geometries corresponding to local minima in energy, determined by MNDO [14]. The conformers are designated by the values of χ_1, the torsional angle about the C^{α}–C^{β} bond, for the two tyrosyl residues. The heat of formation predicted by MNDO is given in parenthesis for each conformer.

states with the $\pi\pi^*$ excited states, under the influence of the static field of the solute only, and of both the solute and water. In the latter case, the vibronic monopoles were also included for the L_b and L_a bands.

For each recorded structure along the trajectory, the rotational strengths were calculated as described. For each structure, a CD spectrum was calculated by placing Gaussian bands of the calculated intensities at the calculated wave-

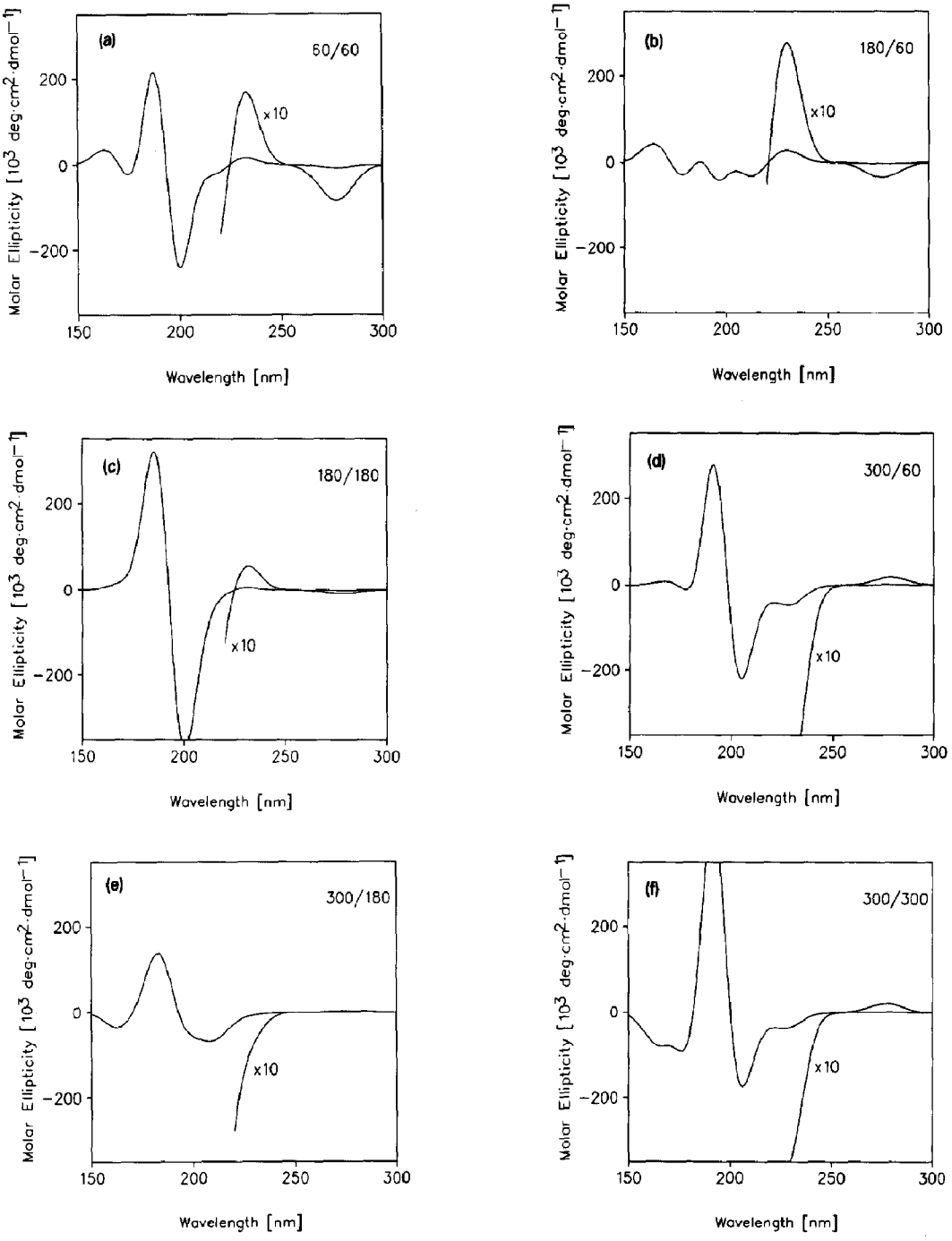

Fig. 3. The calculated CD spectra for the conformers shown in Fig. 2.

lengths, assuming bandwidths of 6.33 nm, 7.00 nm and 8.00 nm for bands in the 150–180 nm, 180–235 nm and 235–300 nm regions, respectively. These bandwidths are smaller by a factor of 2/3 than those observed [9] and commonly used to calculate the spectra for individual structures. The use of a smaller bandwidth in this case takes into account the fact that part of the bandwidth results from variations in the transition energies among individual structures and their interactions with solvent, which are taken into account in our MD simulations. The calculated CD spectra were then averaged over the trajectory to obtain a spectrum for comparison with experiment.

Graphic representations of molecular structures utilized an interactive program, SCHAKAL [28].

3. Results and discussion

The six conformers resulting from variation in the dihedral angle χ_1 of the tyrosyl side chains are shown in Fig. 2. These conformers have been subjected to energy minimization by MNDO/MOPAC [14]. The values for the enthalpy of formation are shown with each structure in Fig. 2 and are also given in Table 1. By this criterion, the (300, 300) conformer is the most stable form in vacuo, with the (300, 60) and (300, 180) conformers less stable by ≈ 6 and 4 kJ/mol, respectively. The doubly folded conformer (60, 60) is least stable, 13 kJ/mol above the minimum energy conformer.

Table 1

MNDO and GROMOS energies of conformers

Conformer [a]	ΔH_f^{MNDO} (kJ/mol)	E_{pot}^{GROMOS} (kJ/mol)
(60, 60)	−478.66	91.35
(180, 60)	−483.53	96.44
(180, 180)	−484.21	100.27
(300, 60)	−486.34	99.74
(300, 180)	−488.10	95.95
(300, 300)	−492.10	96.64

[a] Each conformer was first subjected to energy minimization using MNDO [14], followed by GROMOS [15]. The energies given for each method refer to the energy following minimization in the corresponding force field.

After energy minimization by GROMOS [15], the order of conformational energies is altered substantially, as shown in Table 1. In terms of potential energy in the GROMOS force field, the (60, 60) conformer is lowest in energy, with the (300, 180), (180, 60) and (300, 300) conformers ca. 5 kJ/mol higher in energy and the (300, 60) and (180, 180) conformers ca. 9 kJ/mol higher.

Figure 3 shows the CD spectra calculated for each of the MNDO energy-minimized conformers. Comparison of these calculated spectra with the experimental [9] spectrum (Fig. 1) shows that the three lowest energy conformers are predicted to have CD spectra which qualitatively agree with the experimental spectrum, giving a positive L_b band, negative L_a and $n\pi^*$ bands, and a strong negative feature near 200 nm. Of these three, the conformer (300, 180) gives the least satisfactory

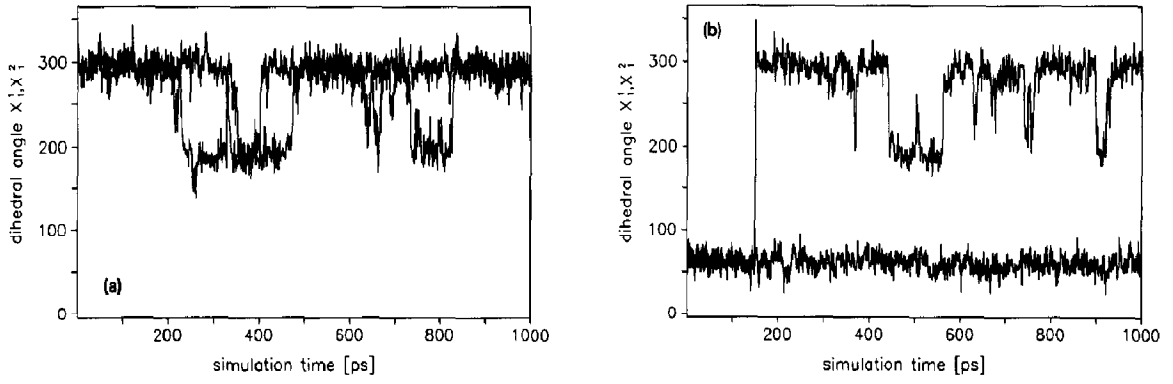

Fig. 4. Time series of χ_1 for the two tyrosyl side chains over the course of two 1000 ps simulations at 300 K. (a) Starting with the (300, 300) conformer. (b) Starting with the (60, 60) conformer.

spectrum, with no discernible L_a and $n\pi^*$ bands but only a broad negative feature culminating in a relatively weak negative feature near 210 nm. The three higher energy conformers all give negative L_b and positive L_a bands, in contrast to experiment. It is interesting to note that all of the conformers except for (180, 60) have a moderate to very strong negative band near 200 nm.

In vacuo MD simulation starting from the (300, 300), (300, 60) and (60, 60) conformers showed no interconversions with other conformers during simulations for as long as 1000 ps. Simulations including solvent molecules were therefore initiated using the lowest (300, 300) and highest (60, 60) energy conformers as starting geometries. In 1000 ps of simulation, each run sampled three different conformers, as shown in Fig. 4, where the two χ_1 values are plotted as a function of time. Thus, for example, the simulation starting at (60, 60) underwent a sharp transition to the (300, 60) conformer at ca. 150 ps, followed by several transitions to the (180, 60) conformer throughout the rest of the simulation, always returning to the (300, 60) conformation. The two simulations each sampled a different set of conformers. Ideally, we would wish to have all six conformers sampled in a single run, as this would provide the most reliable averaging of properties. However, from the two 1-ns simulations done thus far, it seems likely that simulations for tens of ns would be required to assure complete sampling of conformational space in a single run.

Table 2

Average potential energies and frequencies of conformers during simulations

Conformer	Average potential energy [a]		Relative frequency
	Partial [b]	Total [c]	
Simulation starting with (60, 60) conformer			
(60, 60)	−198.4	−15484	0.150
(180, 60)	−198.8	−15496	0.166
(300, 60)	−200.3	−15504	0.684
Simulation starting with (300, 300) conformer			
(180, 180)	−201.0	−15498	0.051
(300, 180)	−199.9	−15494	0.309
(300, 300)	−205.5	−15503	0.640

[a] In kJ/mol.

[b] Solute plus solute–water interactions.

[c] Including water–water interactions.

Table 2 shows the relative frequency and the average potential energy of the six conformers in the simulations. The conformers (300, 300) and (300, 60), which have the lowest energies as isolated molecules, are the prevalent conformers in the simulations starting from (300, 300) and (60, 60), respectively. Although these conformers are the dominant conformers in the two simulations and have the lowest potential energy *in vacuo* and in simulations in an aqueous environment, the relative abundance of other conformers does not always exhibit a simple relationship to potential energy. For example, in the simulation starting with the (300, 300) conformer, the (180, 180) conformer has the lowest frequency, but is intermediate in potential energy. Conversely, in the simulation starting with the (60, 60) conformer, this starting conformer and (180, 60) have nearly the same frequency, yet (180, 60) has a potential energy which is significantly more negative than (60, 60). These observations underline the dangers of using only potential energy to predict the relative abundance of conformers, even if the contributions of an aqueous environment are included.

Deviations from planarity in the piperazinedione ring are characterized by the folding angle, β, defined as the dihedral angle between the planes defined by the amide groups [13]. For a planar ring, $\beta = 0°$. Positive values of β correspond to a folding of the piperazinedione ring into a boat form with the C^α–C^β bonds in equatorial or bowsprit positions. Negative values of β lead to the opposite type of boat conformer with the C^α–C^β bonds in an axial or flagpole position. Figure 5 shows the time course of the angle β in the two simulations. In both simulations the solute generally alternated between positive and negative values of β. For the simulation starting with the (300, 300) conformer, the angle β primarily fluctuated about a value of ca. −12°, undergoing occasional excursions to positive values as large as ca. +40°. In the other simulation, the amplitude of the fluctuations was smaller, centered about ca. −7° and +15°, although a few fluctuations extended to +40°.

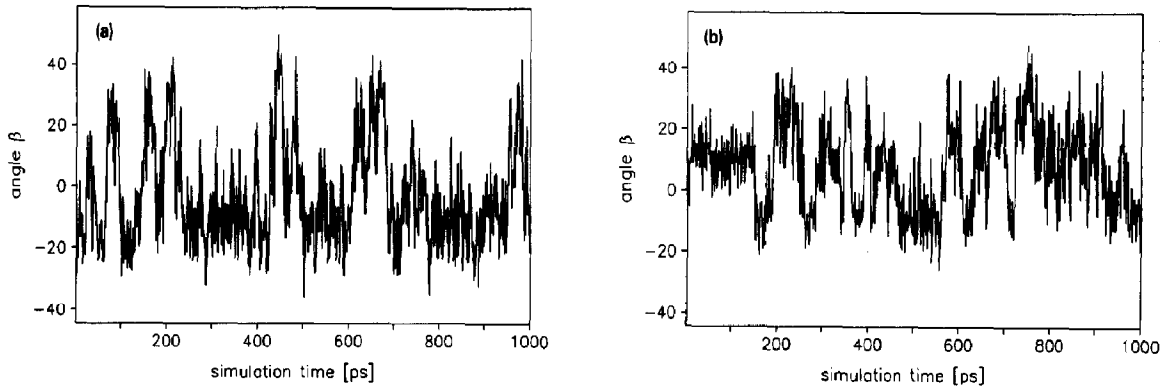

Fig. 5. Time series of the angle β which describes the folding of the piperazinedione ring over the course of two 1000 ps simulations. (a) Starting with the (300, 300) conformer. (b) Starting with the (60, 60) conformer.

Figure 6 summarizes the behavior of the parameter β in a plot of the probability density as a function of β. The simulation starting with the (300, 300) conformer has a simple peak in the probability density at ca. $-12°$, but a long, low shoulder extends to more than $+40°$. Overall, the solute has a preference for negative values of β. In the other simulation, a bimodal distribution was obtained, with peaks at ca. $-7°$ and $+15°$, the latter being larger. Thus, in this simulation, positive β values are dominant.

The CD spectra calculated over the two trajectories, shown in Fig. 7 and Table 3, are similar to each other and to those predicted for the dominant conformers (Fig. 3). Comparison between the spectra calculated with and without inclusion of solvent monopoles shows that the effect of including the solvent static field is small. The effect of including vibronic monopoles for the L_b and L_a bands is also small, as shown in Table 3. The inclusion of $\sigma\pi^*$ states has a significant effect on the L_b rotational strengths, leading to considerably higher ellipticities near 280 nm (1300 deg cm^2/dmole for the (60, 60) trajectory vs. 800 for the equivalent calculation omitting these transitions). The L_a band is decreased somewhat in intensity by including the $\sigma\pi^*$ states, but the overall agreement with experiment is improved.

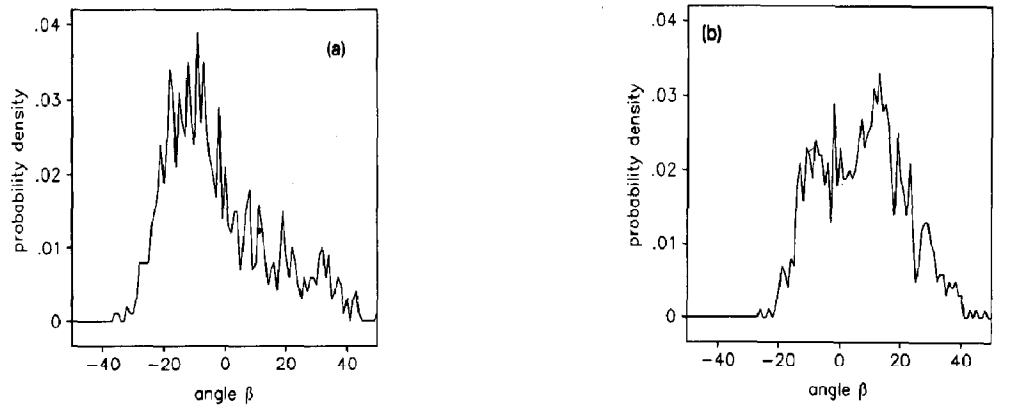

Fig. 6. Probability density for the angle β over the course of two 1000 ps simulations. The probability density is the number of structures within the interval $\beta \pm 0.5°$, divided by the total number of structures recorded in the trajectory (1000). (a) Starting with the (300, 300) conformer. (b) Starting with the (60, 60) conformer.

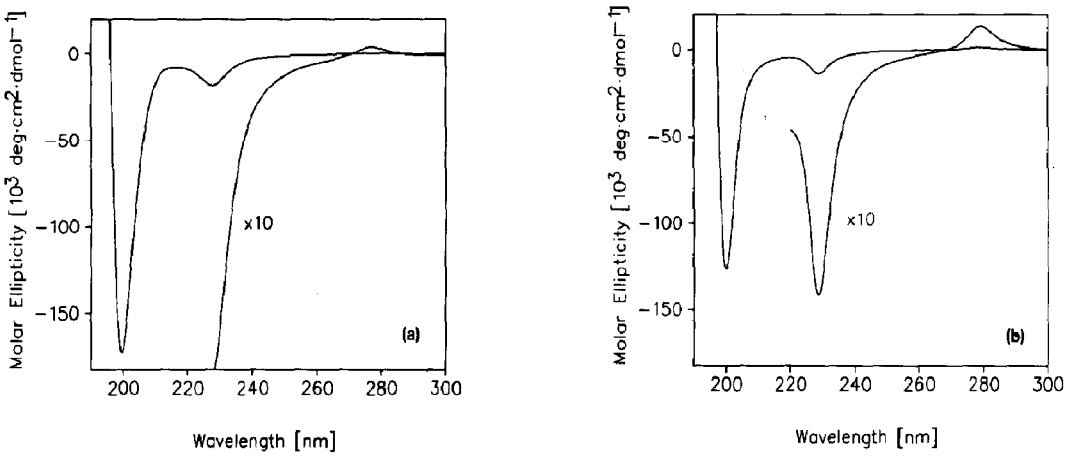

Fig. 7. CD spectra calculated for cYY over the two 1000 ps trajectories, with the inclusion of static field contributions from the solvent, $\sigma\pi^*$ transitions and vibronic monopoles for the L_b and L_a bands. (a) Starting from the (300, 300) conformer. (b) Starting from the (60, 60) conformer.

It is interesting to note that Moscowitz et al. [29] pointed out the possible significance of mixing between the L_b transition and the magnetically allowed $\sigma\pi^*$ transitions for the L_b rotational strength of Tyr, in contrast to Phe where the $\sigma\pi^*$ transitions will lie at much higher energies.

Comparison of the calculated spectra (Fig. 7) with the experimental CD spectrum (Fig. 1) [9] shows good qualitative agreement. The four observed bands are all reproduced with the correct sign. The strong negative band observed near 200 nm shows good agreement in magnitude as well. The features at longer wavelengths, however, are predicted to be significantly weaker than those observed. For example, the L_a band near 230 nm is predicted to have an amplitude of (−14 to

Table 3

Calculated CD band parameters

Wa [a]	SP [b]	VM [c]	Starting conformer	L_b		$L_a + n\pi^*$		$B + \pi\pi^*$	
				λ_{max} [d]	$[\theta]_{max}$ [e]	λ_{max} [d]	$[\theta]_{max}$ [e]	λ_{max} [d]	$[\lambda]_{max}$ [e]
−	−	−	(60, 60)	278.8	0.8	229.1	−12.2	203.3	−124.7
						218.0	−5.7 [f]		
−	−	−	(300, 300)	277.4	0.1	227.3	−18.8	199.1	−179.9
+	−	−	(60, 60)	279.1	0.7	228.6	−12.4	199.4	−145.8
+	−	−	(300, 300)	277.5	0.1	227.3	−18.6	199.1	−180.3
+	−	+	(60, 60)	278.9	0.8	228.8	−18.4	199.4	−137.1
+	−	+	(300, 300)	277.6	0.04	227.4	−21.1	199.1	−174.5
−	+	−	(60, 60)	278.0	1.4	228.3	−13.9	199.1	−125.6
−	+	−	(300, 300)	277.3	0.4	227.5	−15.8	199.6	−176.4
+	+	+	(60, 60)	279.1	1.3	228.7	−14.1	199.9	−126.5
+	+	+	(300, 300)	277.1	0.4	227.6	−18.4	199.5	−172.4

[a] Monopole charges on water molecules included in rotational strength calculation.
[b] $\sigma\pi^*$ transitions included.
[c] Vibronic monopoles for L_b and L_a transitions included.
[d] In nm.
[e] In 10^3 deg cm^2/dmole.
[f] In this case, a discrete negative maximum in the peptide $n\pi^*$ region was predicted.

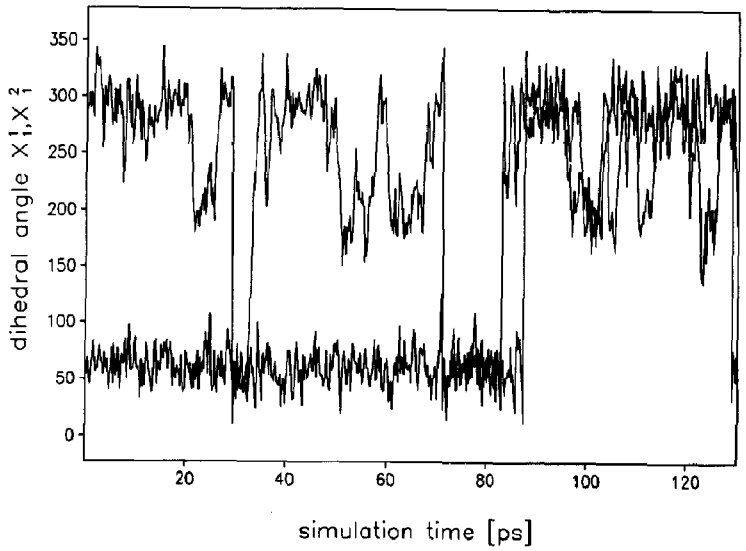

Fig. 8. Time series of χ_1 for the two tyrosyl side chains over the course of a 130 ps simulation at 600 K. Note the transition from a (300, 60) conformer to a (300, 300) conformer which occurs near 90 ps, and from a (300, 300) conformer to a (180, 60) conformer near the end of the simulation.

$-18) \times 10^3$ deg cm^2/dmole, whereas Snow et al. [9] report an amplitude of ca. -70×10^3 deg cm^2/dmole. Similar discrepancies occur for the L_b and the $n\pi^*$ band. The latter band generally shows the largest deviation in magnitude and, in most calculations, is not associated with a discrete negative band.

Two features of the simulations are puzzling at first sight. First, why are no transitions between conformers observed in *in vacuo* calculations on the nano-second timescale, whereas such transitions are observed in the presence of solvent? This result is consistent with results obtained in previous simulations and in conformational energy calculations [30]. In the absence of a solvent, the barriers to interconversion are unrealistically large, and this effect more than compensates for the lack of frictional effects of a solvent.

Second, why are no conformational transitions observed in the presence of water molecules at 300 K between conformers in which one or both χ_1 values are 60° and those for which neither of the χ_1 values are 60°? Interconversions among all six conformers occurred in a 130 ps simulation, including solvent molecules, conducted at 600 K, starting with the (300, 60) conformer (Fig. 8). About 90 ps into this simulation, a transition is observed from a (300, 60) conformer to a (300, 300) conformer. This represents a transition between the two subsets which remained distinct in the two 1-ns simulations at 300 K Several transitions are then observed among the conformers of the second subset, and just before the simulation was terminated, a transition occurred to the (180, 60) conformation, a member of the first subset.

Thus, in this simulation at 600 K, transitions between the two subsets occur on the time scale of ca. 100 ps. If we assume that the free energy of transition state formation is independent of temperature, i.e., the barrier is purely enthalpic, transition state theory predicts a time scale of 200 ns at 300 K. Although the high-temperature simulation is crude, and so is the application of transition state theory, the results show that it is not surprising that in two simulations of 1 ns duration, such transitions have not been observed.

Qualitatively, the barrier for conversion from and to conformers with $\chi_1 \approx 60°$ is expected to be higher than for other conformers because the bulky aromatic ring on C^β lies between the peptide nitrogen and carbonyl carbon substituents on C^α. The conformational energy calculations reported by Snow et al. [9] for cyclo(Ala-Tyr) show a large barrier between the $\chi_1 = 60°$ conformer

and the $\chi_1 = 180°$ and 300° conformers, which are either separated by a low barrier or actually merge into a single minimum.

The existence of two classes of conformers which do not interconvert on the nanosecond timescale at 300 K means that conventional simulations cannot sample all of conformational space within a feasible simulation time. Fortunately, as noted above, our two independent 1-ns simulations yield predicted CD spectra which are very similar. A simulation which indeed sampled all conformational space is therefore expected to closely resemble these two predicted spectra. Further work will be required to obtain a fully satisfactory simulation. Hermans and coworkers [31,32] have developed methods for applying a biasing potential to specific torsional variables (e.g., ϕ and ψ) and obtained free energy differences between different conformations of the Ala dipeptide. This method could be applied to the χ_1^1, χ_1^2 variables in cYY. The free energy differences between the two conformational subsets could be calculated in this way and this would permit the two predicted CD spectra to be combined in the correct way.

In summary, we have shown that molecular dynamics trajectories provide a suitable set of geometries for calculating the circular dichroism spectrum of a moderately flexible model peptide, cYY. The results are in good qualitative agreement with experimental results for the spectrum down to ca. 200 nm, beyond which there are no experimental data. The results also are generally comparable to the previous theoretical results obtained by Boltzmann averaging over a semi-empirical potential energy surface, although these calculations were carried out *in vacuo*. We found that although the solvent did not significantly affect the calculated rotational strengths for a given conformer, it is essential to include the solvent in order to promote transitions among various conformational types. In addition, inclusion of solvent significantly affects the relative energies of the conformational types. Further applications of the present methodology promise to place theoretical calculations of the CD spectra for flexible, solvated molecules on a much sounder footing.

Acknowledgement

This work was supported by grants from the Deutsche Forschungsgemeinschaft (Fl 142/3.1) to JF and AW; the U.S. Public Health Services National Institutes of Health (GM 22994) to RWW; and by a NATO Collaborative Research Grant (880233) to RWW, JF and AW.

References

1 J.A. McCammon and S.C. Harvey, Dynamics of proteins and nucleic acids, (Cambridge University Press, Cambridge, UK, 1987).
2 C.L. Brooks, III, M. Karplus and B.M. Pettit, Adv. Chem. Phys. 71(1988) 1.
3 W.F. van Gunsteren and H.J.C. Berendsen, Angew. Chem. Int. Ed. Engl. 29 (1990) 992.
4 M.J.O. Anteunis, Bull. Soc. Chim. Belg. 87 (1978) 627.
5 A.Yu. Ovchinnikov and V.T. Ivanov, in: The proteins, eds. H. Neurath and R.L. Hill, 3rd edn., vol. 5 (Academic Press, New York, 1982). p. 307.
6 A. Wollmer, J. Fleischhauer, W. Straßburger, H. Thiele, D. Brandenburg, G. Dodson and D. Mercola, Biophys. J. 20 (1977) 233.
7 H. Edelhoch, R.E. Lippoldt and M. Wilchek, J. Biol. Chem. 243 (1968) 4799.
8 E.H. Strickland, M. Wilchek, J. Horwitz and C. Billups, J. Biol. Chem. 245 (1970) 4168.
9 J.W. Snow, T.M. Hooker, Jr. and J.A. Schellman, Biopolymers 16 (1977) 121.
10 K. Bláha and I. Frič, Coll. Czech. Chem. Commun. 35 (1970) 619.
11 J.W. Snow and T.M. Hooker Jr., J. Am. Chem. Soc. 97 (1975) 3506.
12 V. Madison, P.E. Young and E.R. Blout, J. Am. Chem. Soc. 98 (1976) 5358.
13 T.M. Hooker, Jr., P.M. Bayley, W. Radding and J.A. Schellman, Biopolymers 13 (1974) 549.
14 J.J.P. Stewart, QCPE 9 (1990) 581.
15 W.F. van Gunsteren and H.J.C. Berendsen, GROMOS Program System (BIOMOS bv, Laboratory of Physical Chemistry, University of Groningen, Groningen, The Netherlands, 1987).
16 R. Courant. Bull. Am. Math. Soc. 49 (1943) 1.
17 H.J.C. Berendsen, J.P.M. Postma, W.F. van Gunsteren and J. Hermans, in: Intermolecular forces, ed. B. Pullman (Reidel, Dordrecht, The Netherlands, 1981) p. 331.
18 J.P. Ryckaert, G. Cicotti and H.J.C. Berendsen, J. Comput. Phys. 23 (1977) 327.
19 H.J.C. Berendsen, J.P.M. Postma, W.F. van Gunsteren, A. DiNola and J.R. Haak, J. Chem. Phys. 81 (1984) 3684.
20 P.M. Bayley, E.B. Nielsen and J.A. Schellman, J. Phys. Chem. 73 (1969) 228.

21 E. Zobel, Diplomarbeit, RWTH Aachen (1989).
22 B. Kramer, Dissertation, RWTH Aachen (1991).
23 I. Tinoco Jr., Adv. Chem. Phys. 4 (1962)113.
24 J. Downing, Program Package DZDO/MCD3SP (Dept. of Chemistry and Biochemistry, University of Colorado, Boulder, CO, USA, 1986).
25 J.R. Platt, J. Chem. Phys. 17 (1949) 484.
26 N. Sreerama, M.C. Manning and R.W. Woody, Proc. 4th Int. Conf. CD, Bochum, Germany (1991) p. 186.
27 A.D. McLachlan, J. Mol. Biol. 128 (1979) 49.
28 E. Keller. SCHAKAL 88 (© 1988 Kristallographisches Institut, Albert-Universität, Freiburg, Germany, 1988).
29 A. Moscowitz, A. Rosenberg and A.E. Hansen, J. Am. Chem. Soc. 87 (1965) 1813.
30 C.L Brooks, III, M. Karplus and B.M. Pettit, Adv. Chem. Phys. 71 (1988) 177.
31 A. Anderson, M. Carson and J. Hermans, Ann. N.Y. Acad. Sci. 482 (1986) 51.
32 A.G. Anderson and J. Hermans, Proteins Struct. Funct. Genet. 3 (1988) 262.